Analytical ansatz for self-consistent calculations of x-ray transmission and reflection coefficients at graded interfaces

I. D. Feranchuk,[1] S. I. Feranchuk,[1] L. Komarov,[1,*] S. Sytova,[1] and A. Ulyanenkov[2]
[1]*Byelorussian State University, Franciska Skariny Avenue, 4, 220050 Minsk, Republic of Belarus*
[2]*Bruker AXS, Östliche Rheinbrückenstrasse 50, 76187 Karlsruhe, Germany*
(Received 23 January 2003; published 23 June 2003)

We propose a particular analytical representation (ansatz) for analytical solution of Maxwell's equations with one-dimensional potential. The resulting expressions are presented as self-consistent equations for the calculation of x-ray reflection and transmission coefficients at the interfaces with an arbitrary potential profile. The reported approach is testified for typical model potentials, and the convergence of the successive iterations for improvement of solution accuracy is demonstrated. The equations derived in the paper can be used for the solution of the inverse problem in x-ray reflectometry.

DOI: 10.1103/PhysRevB.67.235417 PACS number(s): 61.10.Kw, 61.10.−i, 68.35.Ct

I. INTRODUCTION

The calculation of reflection $R(q)$ and transmission $T(q)$ coefficients of x-ray scattering from interfaces as a function of the normal component of the wave vector q is an indispensable part of the theoretical interpretation of experimental x-ray reflectivity and diffuse scattering data.[1] For sharp ideal interfaces, the analytical expressions for reflection r_s and transmission t_s are similar to Fresnel formulas in optics.[2] These expressions are used, for example, as a primary approximation in distorted-wave Born approximation (DWBA) describing the scattering of x ray from imperfect structures. However, real interfaces have the roughness, grating, or transition layers,[3] which essentially modify the coefficients R and T. There are numerous ways to take this fact into account when simulating x-ray reflectivity (see, e.g., Ref. 3). The common approach is based on the averaging of the real interface structure over the lateral direction. Then the part of the scattering potential related to the averaged structure is proportional to the whole interface surface and gives the main contribution to the reflected wave field. The remaining part of the potential can be taken into account in the framework of DWBA. Thus, in the zeroth approximation, the one-dimensional wave equation has to be solved with a complicated profile of the averaged electron density in the transition layer. The most direct method is to use recurrent Parratt's equations,[4] which deliver a solution of the one-dimensional wave equation for arbitrary interface profile and with required numerical precision. The numerical simulation of wave field, however, requires large computer resources, when diffusely scattered intensity from multilayered structures has to be calculated.[5] The numerical results obtained by solving the direct problem do not allow to construct the model-free algorithms for the inverse problem[6] because of the lack of analytical relations between reflection coefficient and electron density profile. Therefore, the applied x-ray reflectometry uses different approximate models for transition layer at interface and renormalizes the reflection coefficient by the Debye-Waller factor. The simplest form of this factor is a kinematical Rayleigh approximation,[1]

$$R_{DW}=r_s e^{-2q^2\sigma^2}, \tag{1}$$

with a single parameter σ, characterizing the effective width of the transition layer. Another recognized renormalization of the reflection coefficient has been proposed by Nevot and Croce[7] and corresponds to the statistical error function distribution of interface nonuniformity:

$$R_{NC}=r_s e^{-2qp\sigma^2},\quad r_s=\frac{q-p}{q+p},\quad t_s=\frac{2q}{q+p}, \tag{2}$$

where parameter p is determined by the normal component of the wave vector of transmitted wave. The interpolations between both mentioned expressions have been reported in Refs. 8,9. The influence of the transition layer on specular x-ray reflection can also be taken into account by the one-dimensional potential, which permits to find an analytical solution.[3,10]

All the mentioned methods are model dependent and do not allow to establish the relation between electron-density distribution and observed reflection coefficient, which is necessary for the solution of the inverse problem. Therefore, most of the modern approaches to the inverse problem in reflectometry (see, for example Ref. 11) use the formula for reflection coefficient based on the first Born approximation,[12]

$$R_{kin}=r_s\frac{1}{\rho_0}\int_{-\infty}^{\infty}dz\,\frac{d\rho}{dz}e^{i2qz}, \tag{3}$$

where function $\rho(z)$ determines the distribution of electron density within the transition layer and ρ_0 is the density of substrate. However, the applicability of the Born approximation is limited either to the region of large values of moment transfer q, where the reflection coefficient is relatively small, or to the density profiles with small gradients. Moreover, the Born approximation does not describe well enough the phases of the transmission and reflection coefficients, which can essentially distort the solution of the inverse problem. The correct description of wave field phases is also important for the calculation of diffuse x-ray scattering and for interference effects within the multilayered structures. Caticha[13] proposed the self-consistent method for the calculation of $R(q)$ and $T(q)$, which has wider applicability area in comparison with Eq. (3). The drawbacks of this method are the ambiguity of results due to the model of self-consistency and

undefiniteness of algorithm for calculation of high-order approximations for improvement of accuracy. The one-dimensional profile is just an approximate description of the interface structure. Therefore, the solution accuracy for the one-dimensional wave equation does not play a crucial role for very rough interfaces, because in this case the successive DWBA corrections are comparable with the precision of the zeroth approximation.

Nevertheless, the theory expressing the functions $R(q)$ and $T(q)$ through the potential of the one-dimensional transition layer for arbitrary value of q without additional parametrization and out of the framework of perturbation theory has a promising perspective for many applications. In the present paper, a different approach, further called SCA (self-consistent approach), for the self-consistent calculation of the reflection and transmission coefficients is reported. The expressions obtained establish the analytical though nonlinear relation between the scattered x-ray wave field and density profile of the transition layer (Sec. II). The algorithm is approved for several model potentials and is shown to provide high precision for calculated amplitudes and phases of coefficients $R(q)$ and $T(q)$ (Sec. III). The convergence of high-order approximations is numerically studied, and an asymptotic behavior of coefficients is found for small and large values of q (Sec. IV). Using the proposed analytical ansatz, the measured experimental data on x-ray reflectivity are interpreted. The parameters of sample evaluated by using the SCA and conventional methods for the calculation of reflection coefficients are found to be sometimes essentially different (Sec. V).

II. DERIVATION OF THE BASIC EXPRESSIONS

The wave field $E(z)$ of monochromatic x-ray beam reflected from the substrate with the one-dimensional transition layer on the top is defined by the equation

$$\left[\frac{d^2}{dz^2}+q^2+V\varphi(z)\right]E(z)=0. \tag{4}$$

The z axis is assumed to be perpendicular to the surface of substrate (Fig. 1); the in-plane component of the wave vector is conserved and the normal z component is expressed as $q=k\sin\alpha$ with α being the incidence angle and k being the wave number; function $\varphi(z)$ determines the normalized potential of the transition layer with amplitude $V=k^2\chi_0$, where χ_0 is the complex polarizability of sample material; the conditions $\varphi(-\infty)=0$ and $\varphi(\infty)=1$ are fulfilled.

The integral form of Eq. (4) is

$$E(z)=Ae^{iqz}+Be^{-iqz}+\frac{V}{2iq}\left[e^{iqz}\int_z^\infty dz' e^{-iqz'}\varphi(z')E(z')\right.$$
$$\left.+e^{-iqz}\int_{-\infty}^z dz' e^{iqz'}\varphi(z')E(z')\right]. \tag{5}$$

Direct iterations of this equation with constants A and B following from the boundary conditions result in the Born series of perturbation theory, which is convergent not for all values of system parameters. The self-consistent approach[13] for the solution of Eq. (5) assumes the use of some approximate form $E_0(z)$ for function $E(z)$ and finding parameters for this form by Eq. (5). Specifically, in Ref. 13, function $E_0(z)$ has been taken as the solution of wave equation for sharp interface with variable position z_0 of interface. This solution improves essentially the perturbation theory, but does not eliminate the ambiguity in the reflection and transmission coefficients because of the dependence on the self-consistency mode. Moreover, it does not allow to calculate the successive corrections for the zeroth approximation.

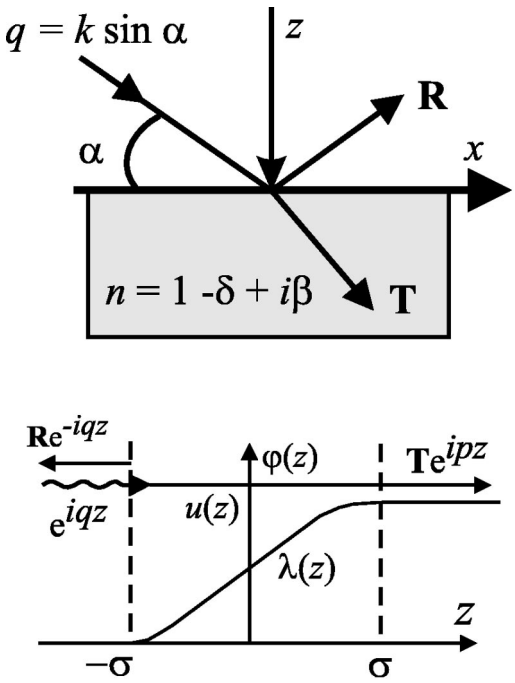

FIG. 1. Sketch of scattering geometry and wave field distribution in the transition layer.

To formulate the basics of the SCA, the potential function and solutions are redefined in the following way (Fig. 1):

$$\varphi(z)=H(z-\sigma)+\lambda(z)H(\sigma-z)H(z+\sigma),$$
$$E(z)=H(-z-\sigma)[e^{iqz}+Re^{-iqz}]+u(z)H(\sigma-z)H(z+\sigma)$$
$$+H(z-\sigma)Te^{ipz}. \tag{6}$$

Here $H(z)$ is the Heaviside function; $\lambda(z)$ is a potential function varied from zero to unity inside the transition layer located between the planes with coordinates $\pm\sigma$ (in most general case $\sigma\to\infty$); coefficients R and T in function $E(z)$ are the exact coefficients of reflection and transmission. By definition, function $E(z)$ describes the transmitted wave at $z=+\infty$ if the condition is satisfied:

$$p^2=q^2+V. \tag{7}$$

The function $u(z)$ is defined within the interval $|z|<\sigma$ and satisfies the boundary conditions at $z=\pm\sigma$, as follows from the discontinuity condition for the solution:

$$u(\sigma)=Te^{ip\sigma},\quad u(-\sigma)=Re^{iq\sigma}+e^{-iq\sigma}. \tag{8}$$

Substituting Eq. (6) into Eq. (5), we derive the relationship

$$Ae^{iqz}+Be^{-iqz}+\frac{V}{2iq}e^{iqz}\left[\int_{-\sigma}^{\sigma}d\xi e^{-iq\xi}\lambda(\xi)u(\xi)+\int_{\sigma}^{\infty}d\xi e^{-iq\xi}Te^{ip\xi}\right]=e^{iqz}+Re^{-iqz},$$

$$z<-\sigma,$$

$$Ae^{iqz}+Be^{-iqz}+\frac{V}{2iq}\left\{e^{-iqz}\left[\int_{-\sigma}^{\sigma}d\xi e^{iq\xi}\lambda(\xi)u(\xi)+\int_{\sigma}^{z}d\xi e^{iq\xi}Te^{ip\xi}\right]+e^{iqz}\int_{z}^{\infty}d\xi e^{-iq\xi}Te^{ip\xi}\right\}=Te^{ipz},$$

$$z>\sigma,$$

$$Ae^{iqz}+Be^{-iqz}+\frac{V}{2iq}\left[e^{iqz}\int_{\sigma}^{\infty}d\xi e^{-iq\xi}Te^{ip\xi}+e^{iqz}\int_{z}^{\sigma}d\xi e^{-iq\xi}\lambda(\xi)u(\xi)+e^{-iqz}\int_{-\sigma}^{z}d\xi e^{-iq\xi}\lambda(\xi)u(\xi)\right]=u(z),$$

$$-\sigma<z<\sigma. \tag{9}$$

Equating the coefficients at fast-oscillating exponents in both parts, the constants are found to be $A=0$, $B=R$, whereas the reflection and transmission coefficients and the function $u(z)$ should be defined from the following equations:

$$R+\frac{VT}{2q(p+q)}e^{i(p+q)\sigma}+\frac{V}{2iq}\int_{-\sigma}^{\sigma}d\xi e^{iq\xi}\lambda(\xi)u(\xi)=0,$$

$$\frac{VT}{2q(p-q)}e^{i(p-q)\sigma}+\frac{V}{2iq}\int_{-\sigma}^{\sigma}d\xi e^{-iq\xi}\lambda(\xi)u(\xi)=1,$$

$$u(z)=Re^{-iqz}+\frac{VT}{2q(p-q)}e^{i(p-q)\sigma}e^{iqz}+\frac{V}{2iq}\int_{-\sigma}^{\sigma}d\xi[e^{iq(z-\xi)}H(\xi-z)+e^{-iq(z-\xi)}H(z-\xi)]\lambda(\xi)u(\xi). \tag{10}$$

The system of equations (10) for function $u(z)$ along with boundary conditions (8) is the exact consequence of primary integral equation. However, the advantage of it is the implicit form of fast-oscillating terms in equations, which permits to solve the integral equation for function $u(z)$ within the limited interval, and the latter function is parametrized mainly by the potential function $\lambda(z)$. To approximately calculate the self-consistent values $R(q)$ and $T(q)$, some model form (ansatz) for function $u(z)$ has to be chosen. This model function is expected to satisfy the following conditions: (i) its variation is mainly determined by the potential function, (ii) it satisfies boundary conditions (8), (iii) it does not include any additional parameters. The simplest representation of $u(z)$, fulfilling the mentioned conditions, is

$$u_0(z)=\lambda(z)Te^{ipz}+[1-\lambda(z)](Re^{-iqz}+e^{iqz}). \tag{11}$$

Ansatz (11) is the basic expression of the SCA and it can be considered as the zeroth-order iteration for the solution of integral Eq. (10). The substitution of this ansatz into Eq. (10) results in self-consistent equations for the calculation of the reflection and transmission coefficients through the potential function:

$$\left[1-i\frac{VK(0)}{2q}\right]R(q)+\frac{VL(p+q)}{q(p+q)}T(q)=i\frac{VK(2q)}{2q},$$

$$-i\frac{VK(-2q)}{2q}R(q)+\frac{VL(p-q)}{q(p-q)}T(q)=1+i\frac{VK(0)}{2q},$$

$$K(r)=\int_{-\sigma}^{\sigma}dze^{irz}\lambda(z)[1-\lambda(z)],$$

$$L(r)=\int_{-\sigma}^{\sigma}dze^{irz}\lambda(z)\lambda'(z), \tag{12}$$

from which the result for the zeroth-order approximation follows:

$$R(q)=\frac{iV^2[K(2q)L(p-q)(p+q)-K(0)L(p+q)(p-q)]-2qVL(p+q)(p-q)}{iV^2[K(-2q)L(p+q)(p-q)-K(0)L(p-q)(p+q)]+2qVL(p-q)(p+q)},$$

$$T(q)=\frac{V^2[K^2(0)-K(2q)K(-2q)]+4q^2}{iV^2[K(-2q)L(p+q)(p-q)-K(0)L(p-q)(p+q)]+2qVL(p-q)(p+q)}. \tag{13}$$

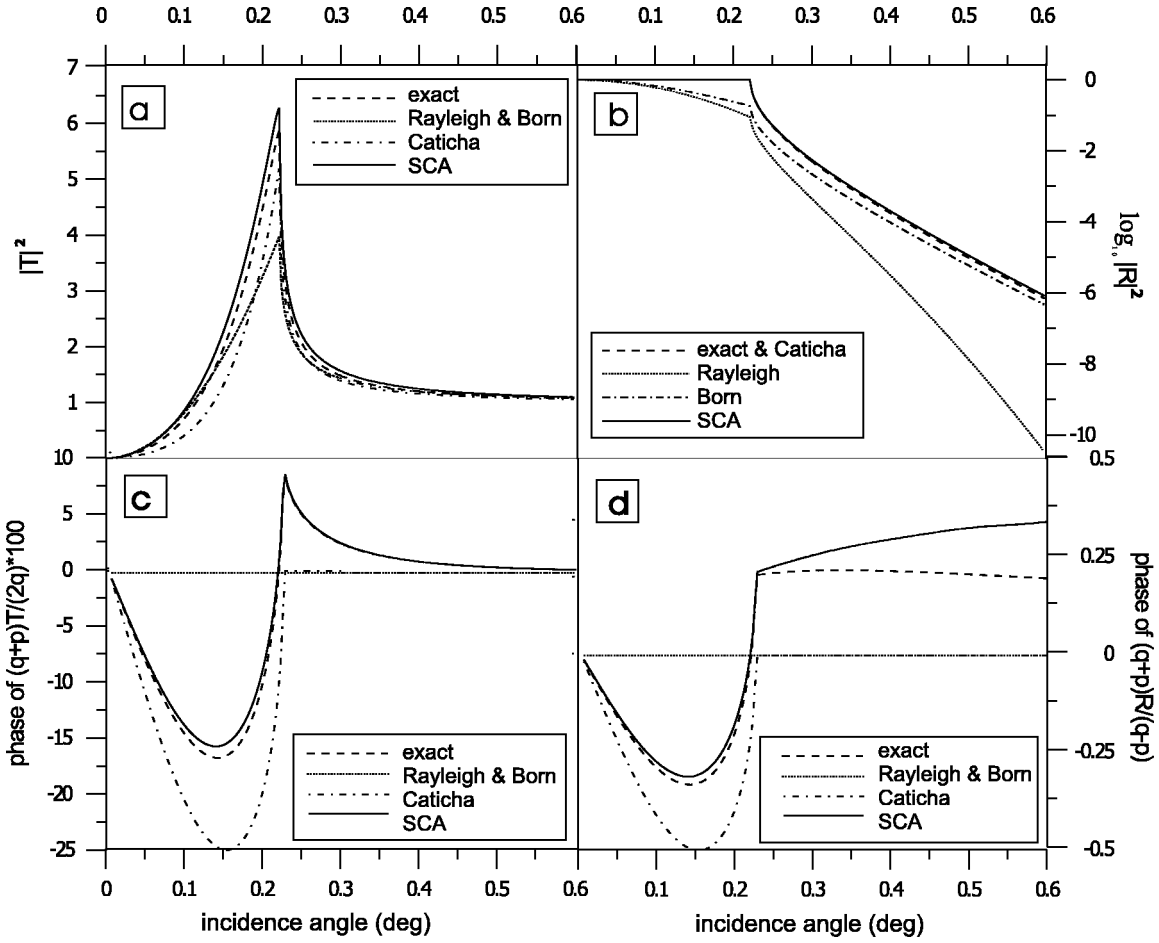

FIG. 2. Reflection (decimal logarithmic base) and transmission coefficients and their phases (in radians) calculated by different methods for the Epstein profile.

Equation (13) confirms the fact that the self-consistent calculation of the reflection and transmission coefficients permits to express them directly through the density profile of the transition layer, though this relation is more complicated than that for the Born approximation. The successive approximations for the coefficients can be easily found because Eq. (13) is obtained from the exact integral equation for function $u(z)$. The procedure for finding $u^{(1)}(z)$ is the following: Eq. (10) is iterated and new solutions are substituted into the expressions for the reflection and transmission coefficients (see Sec. IV for details). However, the zeroth approximation is proved below to be very accurate and sufficient for experimental data interpretation.

III. NUMERICAL RESULTS FOR MODEL POTENTIALS

In this section, the zeroth approximation of the SCA is compared with the exact solutions for several model potentials. The Epstein profile[10] is the most frequently used analytical potential for modeling of the transition layer. The potential function corresponding to this potential is [the parameter σ in Eq. (6) is assumed to be equal to infinity]

$$\varphi(z)=\tfrac{1}{2}[1+\tanh(z/\sigma_E)]. \tag{14}$$

Exact formulas for the coefficients are well known for this case (see, e.g., Ref. 3):

$$R(q)=-\frac{q+p}{q-p}\frac{\Gamma(iq\sigma_E)}{\Gamma(-iq\sigma_E)}\frac{\Gamma^2[-i(q+p)\sigma_E/2]}{\Gamma^2[i(q-p)\sigma_E/2]},$$

$$T(q)=\frac{q+p}{2p}\frac{\Gamma^2[-i(q+p)\sigma_E/2]}{\Gamma(-iq\sigma_E)\Gamma(-ip\sigma_E)}, \tag{15}$$

and integrals from Eq. (13) are expressed for this potential analytically:

$$K(r)=\frac{\pi\sigma_E^2 r}{4\sinh(\pi\sigma_E r/2)},\quad L(r)=\frac{\pi\sigma_E r(1+i\sigma_E r/2)}{4\sinh(\pi\sigma_E r/2)}. \tag{16}$$

Figures 2(a)–2(d) show the simulations of the reflection and transmission coefficients and their phases (in radians) by various methods: (i) exact, (ii) Rayleigh approximation (1), (iii) Born approximation (3), (iv) approximation by Caticha,[13] and (v) SCA. For all the cases, the values for sample parameters correspond to silicon substrate: $\mathrm{Re}\chi_0=-1.512\times10^{-5}$, $\sigma_E=49$ Å, CuK_α radiation. The large value

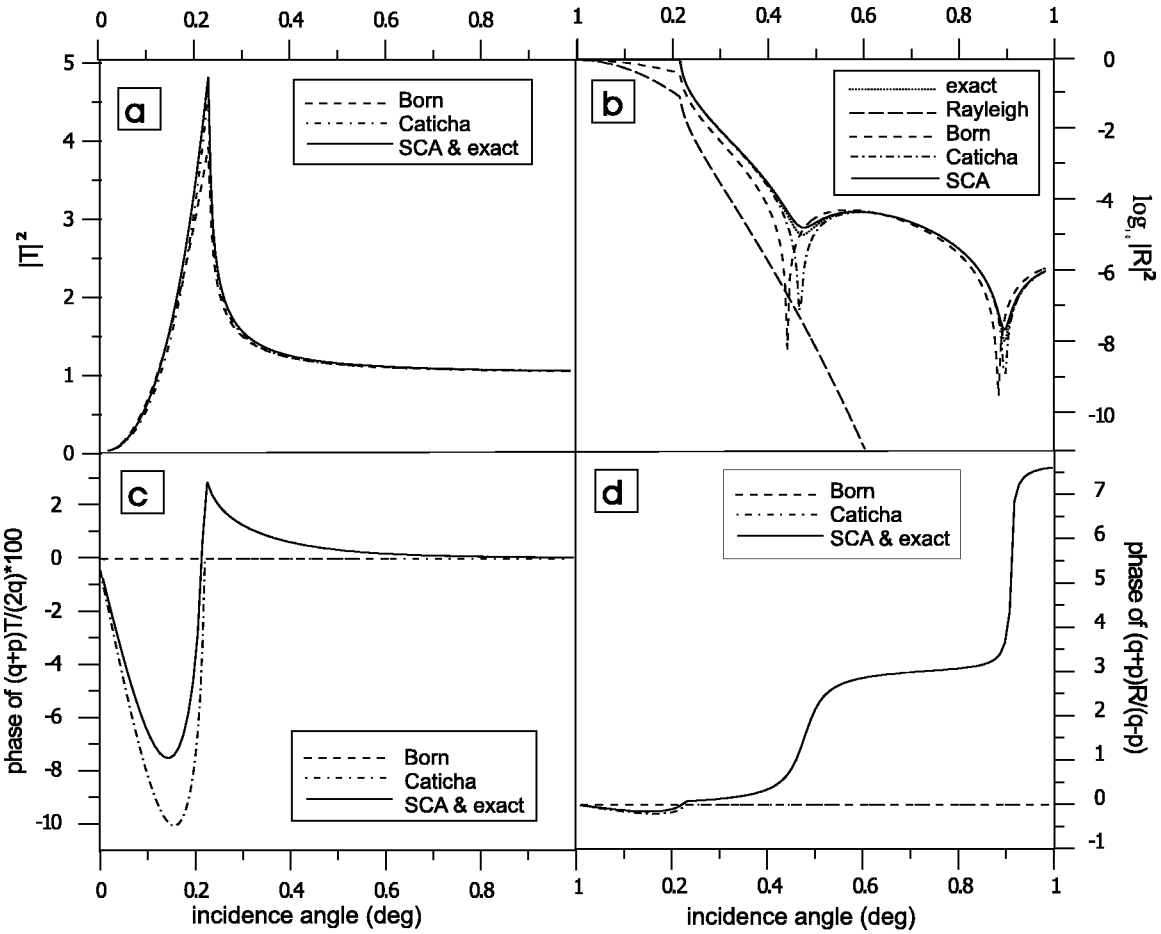

FIG. 3. Reflection (decimal logarithmic base) and transmission coefficients and their phases (in radians) calculated by different methods for the linear profile.

of σ_E for the transition layer width is used in order to compare various methods out of the framework of the perturbation theory.

Figure 2 shows that the functions $R(q)$, $T(q)$ are incorrectly simulated when using phenomenological (Rayleigh) and Born approximations, whereas both self-consistent solutions (Caticha and SCA) fit well to the exact one for the reflected intensity [Fig. 2(b)]. However, the difference between the latters is essential for the intensity of the transmitted radiation [Fig. 2(a)] and especially for the phases of both coefficients [Figs. 2(c) and 2(d)]. Thus, the only proposed SCA, in the paper, provides the best description for all of the scattering characteristics. The same comparison is shown in Figs. 3(a)–3(d) for the linear transition layer:

$$\lambda(z)=\frac{1}{2\sigma}(z+\sigma). \tag{17}$$

The latter model differs qualitatively from the Epstein profile because of the discontinuity of the potential function derivative at the boundaries of the transition layer. However, this model is closer to the real graded interfaces, because the continuity of derivatives at the boundaries results in the exponentially small, nevertheless, nonzero density value at the infinite distances from the sample, which is not correct from the physical point of view. The solution for wave equation with potential (17) can also be represented analytically through the Airy functions Ai and Bi (Ref. 14) on interval $[-\sigma,\sigma]$:

$$u(z)=C_1 Ai(\mu z-a)+C_2 Bi(\mu z-a),$$

$$\mu=\left(-\frac{V}{2\sigma}\right)^{1/3}, \quad a=\frac{V}{2\lambda^2}. \tag{18}$$

Then the coefficients $C_{1,2}$ and $R(q)$, $T(q)$ are found as the solutions of algebraic equation system following from the continuity conditions at the boundaries of the transition layer:

$$e^{-iq\sigma}+R(q)e^{iq\sigma}=C_1 Ai(-\mu\sigma-a)+C_2 Bi(-\mu\sigma-a),$$

$$iq[e^{-iq\sigma}-R(q)e^{iq\sigma}]$$

$$=\mu[C_1 Ai'(-\mu\sigma-a)+C_2 Bi'(-\mu\sigma-a)],$$

$$T(q)e^{iq\sigma}=C_1 Ai(\mu\sigma-a)+C_2 Bi(\mu\sigma-a),$$

$$iqT(q)e^{iq\sigma}=\mu[C_1 Ai'(\mu\sigma-a)+C_2 Bi'(\mu\sigma-a)]. \tag{19}$$

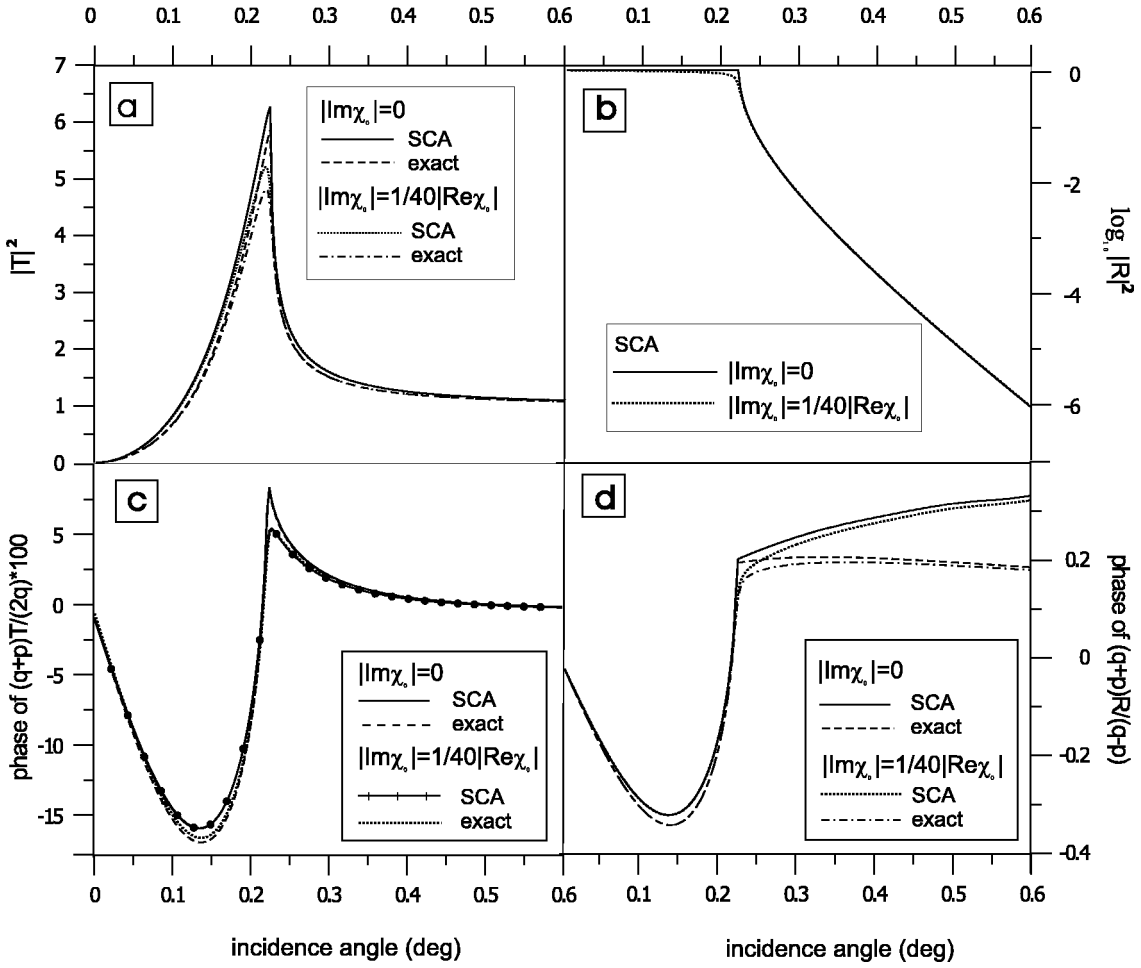

FIG. 4. Effect of the imaginary part of the x-ray susceptibility on the scattering characteristics.

The integrals for the SCA are calculated analytically in this case:

$$K(r)=\frac{1}{\sigma^2 r^3}(\sin\sigma r-\sigma r\cos\sigma r),$$

$$L(r)=\frac{i}{\sigma^2 r^2}(\sin\sigma r-\sigma r e^{i\sigma r}). \tag{20}$$

The curves in Figs. 3(a–d), simulated at the same parameter values as for the tangential profile, depict the results of the exact, SCA, Born, Rayleigh, and Caticha[13] approximations. The decrease in the reflection coefficient R is slower in the case of the transition layer of finite width (power law) than in the case of the layer with tangential profile (exponential law) at large incidence angles, which corresponds better to the experimental data (see Sec. V). One more specific feature of reflection from the linear graded interface is the set of local minima in $R(\alpha)$, caused by derivative discontinuity at the boundaries of the transition layer. The experimental observation of these local gaps seems to be difficult because they are expected at large angles, where the intensity is pretty low. Besides, in real structures the boundaries of the transition layer are not strictly defined, thus intensity is effectively averaged over these local gaps. Nevertheless, the above shown comparison of different methods for the linear layer is important because it demonstrates that the only proposed self-consistent approach describes, with high accuracy, the fine structure of the x-ray reflectivity.

Figures 4(a–d) show the influence of the imaginary part of the potential on the reflection coefficient and its phase for the Epstein potential and different approximations, ($|\mathrm{Im}\chi_0|=1/40|\mathrm{Re}\,\chi_0|$). One can see that the SCA takes correctly into account the radiation absorption in real medium and conformity with the exact results is even better in this case.

IV. CONVERGENCE OF SUCCESSIVE APPROXIMATIONS

Ansatz (11), proposed as an approximate wave field within the transition layer, is not an exact solution for Maxwell's equations, but it gives a simple functional relation between the wave field and potential. The numerical simulations presented above show reasonable and uniform accuracy of ansatz for the calculation of coefficients $R(q)$ and $T(q)$ in entire range of the system parameters. Nevertheless, the comparison of results by the proposed SCA and exact solution of Maxwell's equations for the wave field is necessary. It seems to be difficult to find a strict mathematical proof for the convergence of successive approximations of the SCA,

and therefore we demonstrate here just a numerical evidence of this convergence. Improvement of ansatz (11) accuracy in the framework of the self-consistent approach is realized by the iterations of the exact integral equations (10). These iterations are defined by recurrent formulas for coefficients $R^{(s)}(q)$ and $T^{(s)}(q)$ and function $u^{(s)}(z)$:

$$R^{(s)}(q)=-\frac{p-q}{p+q}e^{2iq\sigma}+\frac{V}{2iq}\int_{-\sigma}^{\sigma}d\xi\left[\frac{p-q}{p+q}e^{iq(2\sigma-\xi)}-e^{iq\xi}\right]\times\lambda(\xi)u^{(s-1)}(\xi),$$

$$T^{(s)}=\frac{2q(p-q)}{V}e^{-i(p-q)\sigma}\times\left[1-\frac{V}{2iq}\int_{-\sigma}^{\sigma}d\xi e^{-iq\xi}\lambda(\xi)u^{(s-1)}(\xi)\right],$$

$$u^{(s)}(z)=R^{(s-1)}e^{-iqz}+\frac{VT^{(s-1)}}{2q(p-q)}e^{i(p-q)\sigma}e^{iqz}+\frac{V}{2iq}\int_{-\sigma}^{\sigma}d\xi[e^{iq(z-\xi)}H(\xi-z)+e^{-iq(z-\xi)}H(z-\xi)]\lambda(\xi)u^{(s-1)}(\xi), \quad (21)$$

and the exact values are determined as a limit of sequence,

$$R(q)=\lim_{s\to\infty}R^{(s)},$$

where the primary terms are given by approximations (11) and (13). Figure 5 shows the successive approximations, calculated by Eqs. (21) for the transition layer with linear profile (17). The differences between the successive iterations are hardly distinguishable, so quickly they converge to the exact solution, and this fact actually demonstrates the stability of the zeroth approximation. Analogous results are found for other model potentials (not shown here).

The self-consistent approach for the solution of Maxwell's equations presented in this paper is a direct analog of operator method for Schrödinger equation, which is proved to be effective for the solution of many problems of quantum mechanics.[15] The coincidence of the zeroth approximation with the exact solution in limiting cases, where the analytical methods can be used, is shown in Ref. 15 to be an important feature of any uniformly suitable approximation. For the case with an arbitrary potential studied in this paper, such analytical results can be found in two limit cases. The first one is the region of incidence angles less than the critical angle of total external reflection ($q^2<|V|$), where the equation $p=\sqrt{q^2+V}=i\kappa$ is fulfilled. For real potential, the integrals for the SCA are represented as $K(q)=K^*(-q)$, $L(q)=L^*(-q)$, and substitution of these equations into Eq. (13) demonstrates the fulfillment of the SCA zeroth approximation to the exact condition in the considered angular range:

$$|R^{(0)}(q)|^2=1,\ \ q^2<|V|. \quad (22)$$

In the second limit case of large incidence angles ($q^2\gg|V|$), one can use the following estimations for integrals:

$$K(q)=-\frac{i}{q}\left[\int_{-\sigma}^{\sigma}dze^{iqz}\lambda'(z)-L(q)\right],$$

$$L(q)\simeq\frac{e^{iq\sigma}\lambda'(\sigma)}{iq}+O(q^{-2}),$$

$$L(p-q)\simeq\frac{i(p-q)}{2}\left[\sigma-\int_{-\sigma}^{\sigma}dz\lambda^2(z)\right]. \quad (23)$$

Substituting these expressions into Eq. (13), the reflectivity is written as

$$R^{(0)}(q)\simeq\frac{V}{2q^2}\int_{-\sigma}^{\sigma}dze^{2iqz}\lambda'(z),$$

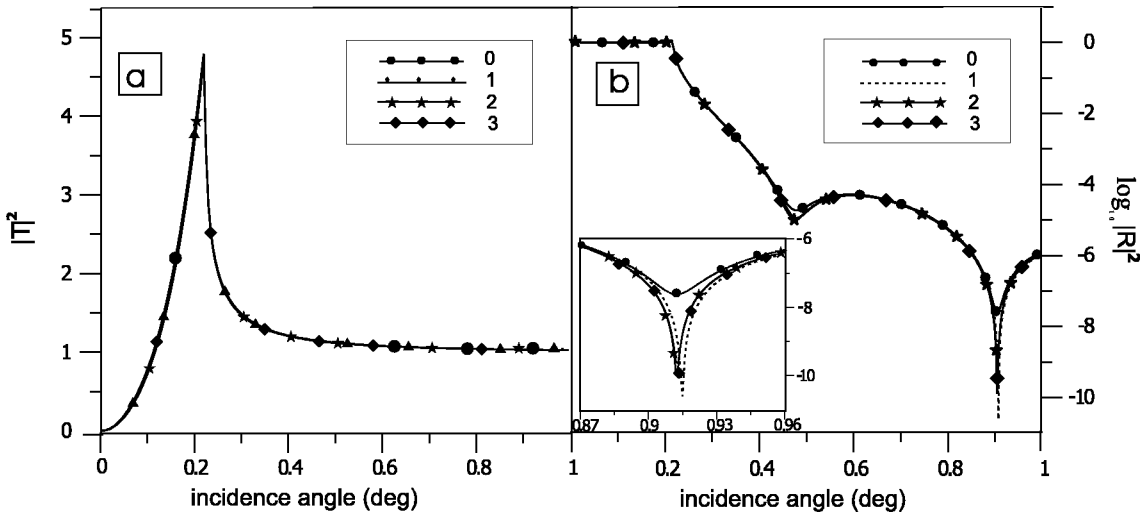

FIG. 5. Convergence of SCA successive approximations for x-ray reflection and transmission coefficients. The inset shows the area, where various approximations have most of the differences. The second and third approximations are indistinguishable.

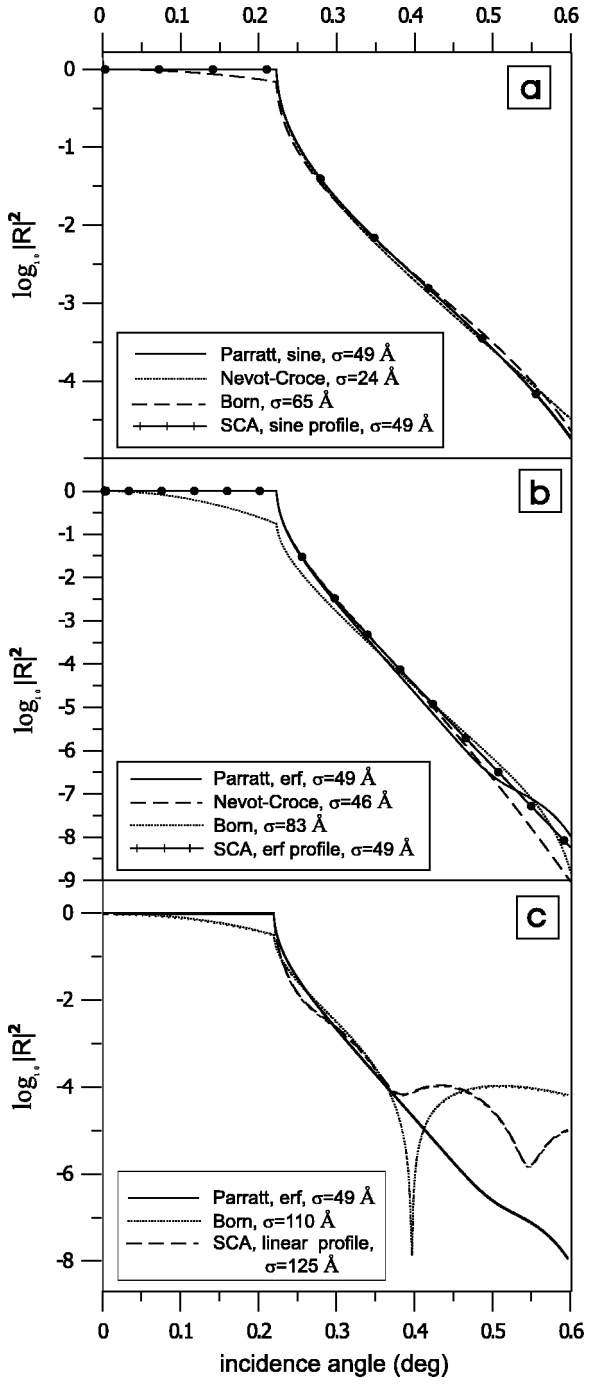

FIG. 6. X-ray reflectivity simulated by classical Parratt's formalism (solid line) and reflectivities by Nevot-Croce, Born, and SCA methods for (a) sinusoidal, (b) error function profiles, and (c) by means of linear model potential (see comments in the text).

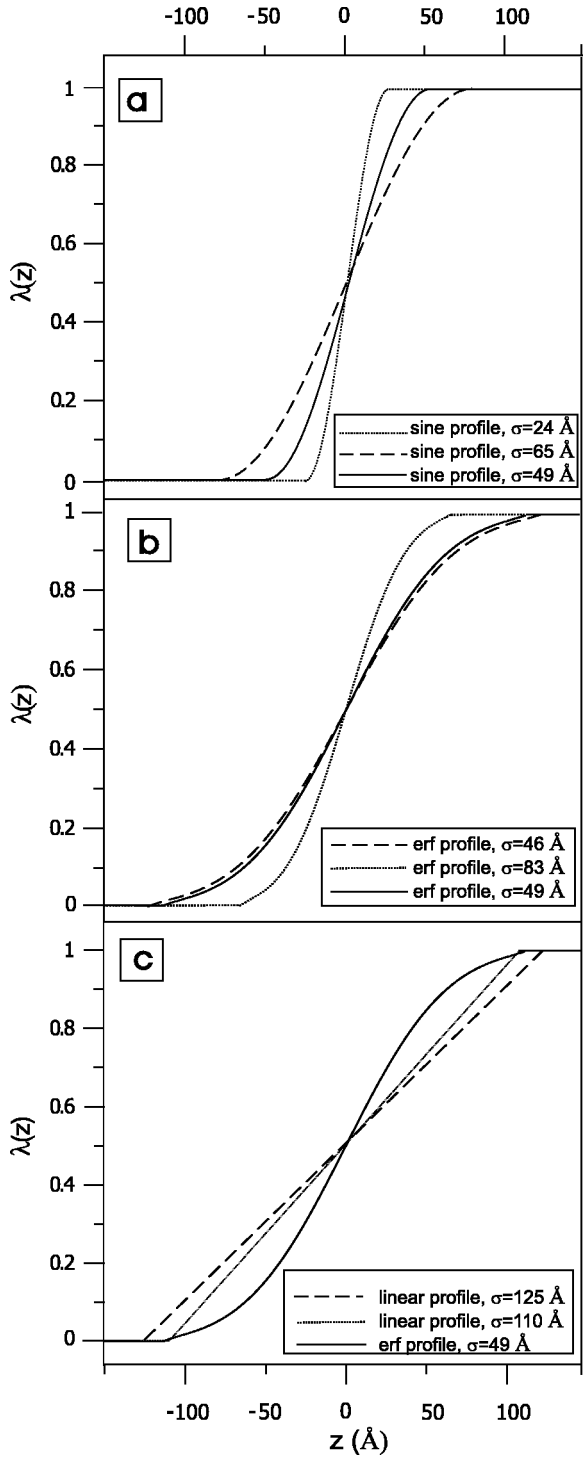

FIG. 7. Inverse problem solutions for (a) sinusoidal, (b) error function profiles with different value of σ, and (c) for linear model profile.

i.e., for large value of q, the SCA zeroth approximation is equivalent to the Born approximation (3), which is asymptotically exact at large angles.

Thus, the proposed ansatz is believed to be a uniformly suitable approximation for electromagnetic wave field, scattered from the one-dimensional graded interface, since it satisfies all the limiting cases and its successive approximations converge to the exact solution. The fast convergence of successive approximations points to the fact that the reflectivity curves in the third and fourth iterations are hardly distinguishable and fit well the exact solution. This fast convergence has been shown[15] to be a specific feature of iterational approach in comparison with the additive correction approach, used in conventional perturbation theory. The convergence rate of successive iterations obtained for x-ray reflectivity in the present work correlates well with the results

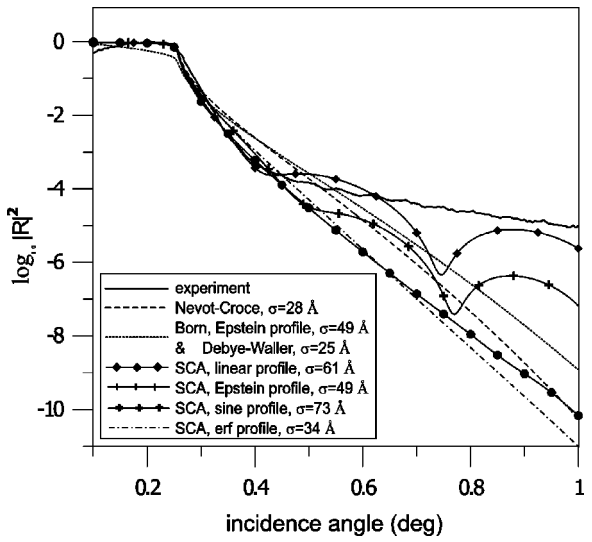

FIG. 8. Measured x-ray reflectivity (solid line) from $Si_{0.65}Ge_{0.35}$ substrate and best fits by different methods.

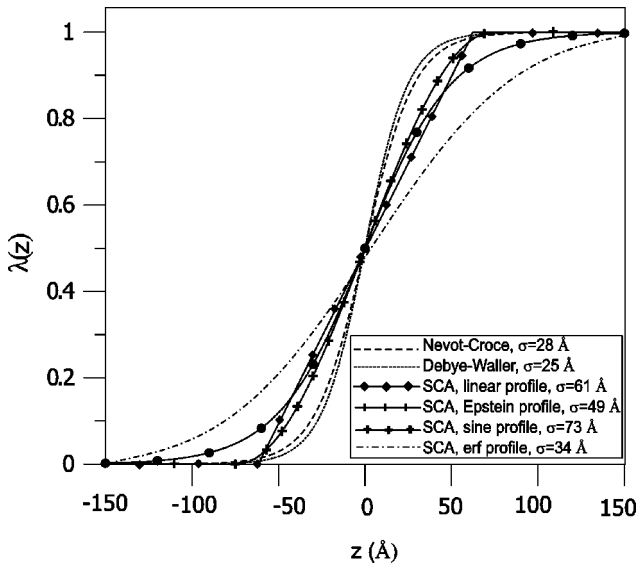

FIG. 9. The potential profiles corresponding to reflectivities simulated in Fig. 8.

of various problems solved by the analogous iteration method (see Ref. 15 and references therein).

V. INTERPRETATION OF THE MEASURED X-RAY REFLECTIVITY

The resulting expressions (11) and (13) derived in this work can be used for both the *direct* (simulation of the scattered intensity from known potential of transition layer) and *inverse* (determination of density profile from x-ray reflectivity[6]) problems. Besides, the diffusely scattered intensity can also be calculated by DWBA using nonperturbative representation (11) for wave field instead of the conventional zeroth approximation based on the solution for sharp interface.[3] To illustrate the sensitivity of the direct problem solution to the model of interface and to the method of simulation, we use two potential profiles, which have no exact solution but are widely used for modeling of the real graded interface, error function profile, and sine profile:

$$\varphi_1(z)=\frac{\chi_0}{2}[1+\Phi(z/\sigma\sqrt{2})],\quad \Phi(x)=\frac{2}{\sqrt{\pi}}\int_0^x dt e^{-t^2},$$

$$\varphi_2(z)=\frac{\chi_0}{2}\left[1+\sin\frac{\pi z}{2\sigma}\right]. \tag{24}$$

The potential $\varphi_2(z)$ takes into account the natural limits of roughness amplitude. For both potentials, we use the functions $R_{1,2}^{num}(\alpha)$ calculated by Parratt's formalism as ''measured'' reflectivities [Figs. 6(a–c), solid lines]. Then various methods for $R_{1,2}(\alpha)$ simulation have been used and the interface parameters for the best fit between the theoretical and measured reflectivities have been found. In such a way, different methods for an approximate solution of the inverse problem for the graded interface are compared. In the self-consistent approach, the following integrals for potential (24) are used:

$$K_2=-\frac{\pi^2\sin q\sigma}{4q(q^2\sigma^2-\pi^2)},$$

$$L_2=\frac{\pi^2}{8}\left[\frac{\sin q\sigma}{(q^2\sigma^2-\pi^2)}-\frac{4\cos q\sigma}{(4q^2\sigma^2-\pi^2)}\right],$$

$$K_1=\frac{2}{iq\sigma\sqrt{2\pi}}\int_0^\infty dz e^{-z^2/2\sigma^2}\Phi(z/\sigma\sqrt{2})\sin(qz),$$

$$L_1=iqK_1. \tag{25}$$

Figures 6(a,b) show that the measured reflectivity can be modeled well by all approximations, however, the conventional methods (Nevot-Croce, Born) give the best fit at the value of parameters σ, which is essentially different than the exact value $\sigma=49$ Å, used for the simulation of measured curve. As a result, there is a noticeable discrepancy [Figs. 7(a,b)] between the original potential profile and the profiles corresponding to the values σ shown in Fig. 6. In opposite, the SCA delivers the correct value of σ, at which the best fit is found.

Figures 6(c) and 7(c) illustrate the opposite side of the problem. The solution of the inverse problem is known to be dependent both on the method of simulation and on the choice of the model potential profile. To illustrate this fact, the reflectivity for the original error function profile has been fitted to the curves simulated by means of Parratt's algorithm, the SCA, and Born approximation, and using the linear profile. The parameter σ being found from the condition of the best fit [Fig. 6(c)] differs from the exact value 49 Å for all methods, but the result of the Born approximation is far out of the experimental accuracy. The comparison of the known measured potential profile and the profiles found by different methods with the same model potential is shown in Fig. 7(c). These results demonstrate that the Born approxi-

mation is not applicable for the solution of the inverse problem, when the graded interface is thick or possesses large roughness.

Finally, Figs. 8 and 9 show the results of the approximate solution of the inverse problem using the experimentally measured, at CuK_α, wavelength x-ray reflectivity from $Si_{0.65}Ge_{035}$ substrate ($\mathrm{Re}\,\chi_0 = 2\times 10^{-5}$). In this example, it is not our goal to obtain a perfect coincidence of the theoretical and experimental curves, which can be reached by taking into account the instrumental function of reflectometer, diffuse x-ray scattering, and background noise of the detector. These factors, being applied to the curve simulated by the SCA, eliminate the long-wave oscillations and result in a very good fit between the measured and simulated curves (not shown here). The aim of Figs. 8 and 9, however, is to demonstrate the essential dependence of reconstructed sample parameters on the choice of both the model profile and the method of simulation. The surface is known to be very rough in this sample and nonperturbative method has to be used to calculate the solution of the direct problem. We tried several methods for the simulation of x-ray reflectivity on the basis of various models for the density profiles of the transition layer. All the models are parametrized by variable σ; the only parameter used to fit the simulated curve to the measured intensity. Figure 8 shows that the phenomenological approximations (Rayleigh, Nevot-Croce) and analytical model profiles with the exponential decrease of the reflection coefficient (error function, Epshtein) do not permit to fit the measured curve in the entire range of the reflection angles. The linear model seems to be most adequate for data description. The x-ray reflectivities for all analytical models have been calculated by using both the SCA and Parratt's formalism. The curves resulting from these two approaches are not distinguishable in the picture, but they noticeably differ from the result of the Born approximation.

Figure 9 shows the density profiles for the considered sample reconstructed on the basis of the methods listed in the picture legend. The figure demonstrates a high sensitivity of the solution of the inverse problem to the choice of the theoretical method and the model for simulation of the direct problem.

VI. CONCLUSIONS

The analytical representation (ansatz) for electromagnetic wave field has been proposed, which describes the scattering of x-ray radiation from the one-dimensional graded interface with arbitrary density profile. This ansatz gives an accurate conformity of x-ray reflectivity spectra to interface density profile in the entire range of the reflection angles and without additional parametrization. The derived expression for wave fields can be used to adequately solve the inverse problem for x-ray scattering as well as to enhance the accuracy of diffuse scattering calculation on the basis of DWBA.

ACKNOWLEDGMENTS

This work was supported by Bruker AXS GmbH and International Science and Technology Center (Grant No. B-626).

*Deceased.

[1] U. Pietsch, V. Holy, and T. Baumbach, *High Resolution X-Ray Scattering from Thin Films and Multilayers* (Springer-Verlag, Heidelberg, 1999).
[2] M. Born and E. Wolf, *Principles of Optics* (Pergamon Press, Oxford, 1959).
[3] S. Dietrich and A. Haase, Phys. Rep. **260**, 1 (1995).
[4] L.G. Parratt, Phys. Rev. **95**, 359 (1954).
[5] V. Holy and T. Baumbach, Phys. Rev. B **49**, 10 668 (1994).
[6] B. Lengeler, Naturwissenschaften **88**, 249 (2001).
[7] L. Nevot and P. Croce, Rev. Phys. Appl. **15**, 761 (1980).
[8] R. Pynn, Phys. Rev. B **45**, 602 (1992).
[9] D.K.G. de Boer, Phys. Rev. B **49**, 5817 (1994).
[10] P.S. Epstein, Proc. Natl. Acad. Sci. U.S.A. **16**, 627 (1930).
[11] K.M. Zimmermann, M. Tolan, R. Weber, J. Stettner, A.K. Doerr, and W. Press, Phys. Rev. B **62**, 10 377 (2000).
[12] J. Als-Nielsen, D. Jacquemann, K. Kjaer, F. Leveiller, M. Lahav, and L. Leseirowitz, Phys. Rep. **246**, 251 (1994).
[13] A. Caticha, Phys. Rev. B **52**, 9214 (1995).
[14] I.S. Gradshtein and I.M. Ryzhik, *Tables of Integrals, Sums, Series and Products* (Nauka, Moscow, 1971).
[15] I.D. Feranchuk, L.I. Komarov, I.V. Nichipor, and A.P. Ulyanenkov, Ann. Phys. (N.Y.) **238**, 370 (1995).